J. Membrane Biol. 146, 15–28 (1995)

The Journal of
Membrane
Biology

© Springer-Verlag New York Inc. 1995

Preparation, Characterization, and Structure of Half Gap Junctional Layers Split with Urea and EGTA

S. Ghoshroy[1,*], D.A. Goodenough[2], G.E. Sosinsky[1]

[1]Rosenstiel Center, Brandeis University, Waltham, MA 02254-9110
[2]Dept. of Cell Biology, Harvard Medical School, Boston MA 02115

Received: 21 November 1994/Revised: 24 February 1995

Abstract. Gap junctions, collections of membrane channels responsible for intercellular communication, contain two paired hemichannels (also called connexons). We have investigated conditions for splitting the membrane pair using urea. We have developed a protocol which consistently splits the gap junction samples with 60–90% efficiency. Our results indicate that hydrophobic forces are important in holding the two connexons together but that Ca^{2+} ions are also important in the assembly of the membrane pair. Greater yields and better structural integrity of split junctions were obtained with a starting preparation of gap junctions which had been detergent treated. Image analysis of edge views of single connexon layers reveal an asymmetry in the appearance of the cytoplasmic and extracellular surface. Cryo-electron microscopy and image analysis of split junctions show that the packing and structural detail of membranes containing arrays of single connexons are the same as for intact junctions, and that the urea treatment causes no gross structural changes in the connexon assembly.

Key words: Intercellular communication — Membrane channel structure — Image analysis — Molecular recognition — Cryoelectron microscopy

Introduction

Intercellular communication between coupled cells is mediated by discrete cell contact domains called gap junctions (Bennett & Goodenough, 1978). Each gap junction contains tens to thousands of membrane channels. Molecules up to 1000 Daltons in size can readily pass through the 10–15 Å pore of the channels, creating a hydrophilic pathway for the transfer of ions, metabolites, and signal molecules. In excitable tissues, transmission of ions via gap junctions is important in the rapid propagation and coordination of electrical signals (Barr et al., 1965). In nonexcitable tissues, the cytoplasmic exchange of molecules through gap junctions is important in the processes of cell metabolic homeostasis, growth and development (*see* reviews by Bennett et al., 1991, Dermetziel, Hwang & Spray, 1990).

Gap junction membrane channels possess a high degree of symmetry (*see* schematic in Fig. 1*A*). Each membrane channel is composed of two oligomers with each of two adjacent tissue cells contributing one oligomer. Each oligomer is called a connexon and, in current models, each connexon is built from six subunits of a single member of the connexin family (Makowski et al., 1977). Connexons are ~65 Å in diameter and are arranged on a hexagonal lattice with lattice constants ranging from 78–90 Å depending on the isolation conditions and detergent extraction procedures used. The two connexons pair to form a tight seal with a 20–30 Å gap between the apposing cell membranes.

The constituent proteins in gap junctions, the connexins (abbreviated by Cx plus the molecular weight), are a multigene family of proteins with a common folding topology (*see* Fig. 1*B* for schematized folding topology). Proteolysis and antibody susceptibility studies have shown that the protein transverses the membrane four times. The N and C termini are located on the cytoplasmic side of the membrane while the extracellular (or gap) side of the membrane contains two amino acid loops. Comparisons of primary amino acid sequences of various connexins have shown that these proteins contain domains with sequences which are conserved and highly

* *Present address:* Department of Biochemistry and Cell Biology, State University of New York, Stony Brook, NY

Correspondence to: G. Sosinsky

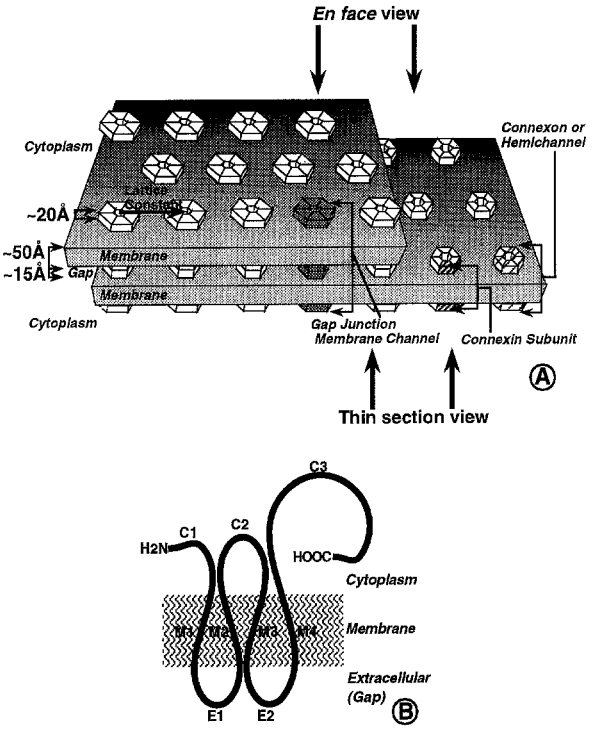

Fig. 1. Model for gap junction structure. Schematic illustration of current models for gap junction structure. (*A*) Each connexon is drawn as a hexamer of connexin subunits. Two apposing connexons dock to form a membrane channel. (*B*) Highly schematized topological folding model of connexin structure containing four membrane spanning domains (M1–M4), two extracellular loops (E1, E2), and three domains localized to the cytoplasmic surface of the membrane (the amino terminus (C1), a cytoplasmic loop (C2) and the carboxy terminus (C3)).

variable. The conserved sequences are localized to the four membrane-spanning domains and the two extracellular loops while the variable amino acid sequences are found in the cytoplasmic domains. Physiological studies using the paired *Xenopus* oocyte expression system have shown that some, but not all connexons composed of different connexins can form an intercellular channel, presumably because the gap portions of the sequence are conserved (Dahl et al., 1987, Swenson et al., 1989).

Gap junctions are isolated as double membrane plaques by membrane fractionation and purification techniques. Three-dimensional structures determined from electron microscopy and X-ray diffraction measurements have led to reconstructions of the membrane pair (Caspar et al., 1977; Makowski, 1988; Unwin & Zampighi, 1980; Unwin & Ennis, 1984; Sikewar & Unwin, 1988; Sikewar et al., 1991). With the exception of recent atomic force microscope images by Hoh et al. (1991, 1993), there is relatively little structural information about the extracellular surfaces of the connexon. These AFM images of the extracellular surface contained subunit detail that was not evident in the three-dimensional reconstructions.

We have investigated conditions for splitting the two membrane bilayers in order to isolate single connexon layers (here, also referred to as split junctions) for further structural analysis. Previous protocols used urea for splitting isolated junction plaques, while gap junctions in tissues were split using hypotonic sucrose (Table 1). However, these procedures gave variable and partial splitting. We have developed a reproducible procedure for splitting isolated rodent liver gap junctions using a combination of urea, chelating agents, and temperature that typically yields a preparation with >70% split junctions when starting with isolated gap junction plaques. We have sought the mildest conditions possible for splitting of the membrane pair to avoid disrupting the junction structure. The conditions of our protocol indicate that hydrophobic interactions are key forces holding the two connexons and that binding of divalent cations between the connexon pairs may also be important. We also present cryo-electron micrographs showing the packing of the connexons in these single layers.

Materials and Methods

Isolation of Rat Liver Gap Junctions

Preparations of isolated gap junctions were made using either an alkali extraction protocol devised by Hertzberg (1984) or a detergent extraction procedure which is detailed in Fallon and Goodenough (1981) and Baker et al. (1985). Protein concentrations of these samples were measured using a colorometric BCA Protein Assay kit (Pierce, Rockford, IL).

Splitting Experiments

In the original splitting procedure devised by Manjunath et al. (1984), pellets of gap junctions were resuspended in a solution containing 8 M urea, 5 mM Tris, pH 10 and were incubated at 37°C for 1 hr. To assess the quality and quantity of split junctions, in our experiments each gap junction preparation of ~0.5 ml was divided into several 0.1 ml "mini-experiments." In all of our experiments, an aliquot of gap junction suspension was added to an aliquot of a urea solution to obtain the desired urea concentration, typically in a 1:1 mixture. The final pH of the mixture was ~ pH 8 rather than pH 10. The protocol that gave good splitting efficiency, quality of membranes and reproducibility was as follows: an aliquot of gap junction suspension in 5 mM Tris and 1 mM EGTA at pH 8 was mixed rapidly by vortexing in a 1:1 ratio with 8 M urea, 5 mM EGTA, 10 mM DTT and 5 mM Tris at pH 10 (final concentrations are 4 M urea, 3 mM EGTA, 5 mM DTT, pH ~8). The sample was then incubated at 37°C for 3 hr and refrigerated at 4°C for about 3–5 days. The sample was centrifuged at high speed to pellet the membranes in an airfuge at 133,000 × *g* or in a TL-100 centrifuge using a TLA100.2 rotor at 280,000 × *g*. The sample was then resuspended in the Tris/EGTA buffer. Results from seven representative experiments using this protocol are listed in Table 3.

Gel Electrophoresis

SDS-PAGE of both intact and split gap junctions was performed according to Goodenough, Paul & Jesaitis, (1988) and our procedure for

immunoblotting followed Francis et al., 1992. The production and characterization of the anti-Cx32 antibody is described in Goodenough et al., (1988) and a description of the anti-Cx26 antibody is found in Goliger and Paul (1994).

Electron Microscopy

Samples that were used for cutting thin sections were pelleted in an airfuge at 133,000 × *g* for 1 hr. To minimize loss of tissue, all fixation and dehydration procedures were done without removing the sample from the airfuge tube. The pelleted membranes were fixed in 2% glutaraldehyde and 1% tannic acid in 0.1 M cacolydate buffer at pH 7.2. Pellets were post-fixed in 1% osmium tetroxide, stained *en bloc* with 1% uranyl acetate, dehydrated in ethanol and acetone and embedded in Epon. Ultrathin sections were made at the silver range (60–70 nm) using an Edgecraft diamond knife on a Reichert Ultracut ultramicrotome. Sections were post-stained with lead citrate. Sections were viewed and images recorded on a Philips 301 electron microscope.

Rat liver gap junctions and split junctions were absorbed to carbon coated grids and stained with 1 or 2% uranyl acetate. Routine negatively stained samples and sections were examined on a Philips 301 microscope. Samples were frozen and cryo-EM images were obtained according to standard low-dose procedures (Dubochet et al., 1981) and recorded on a Philips 420 or CM12 electron microscope equipped with a Gatan 651 anticontaminator and a Gatan 626 cold stage cooled to ≈175°C.

Image Analysis

Images were digitized on an Eikonics CCD model 1412 microdensitometer at a raster of 20 μm (4.44 Å pixel size for images recorded with the Philips 420 or 3.33 Å per pixel for images recorded with the Philips CM12). Correlation averaging of in-plane hexagonal areas were obtained following the procedures described in Sosinsky et al. (1990). In order to obtain a 6-fold average from the correlation averages we used a rotational filtering/power spectrum computer program according to methods outlined in Crowther and Amos (1971). Fourier transforms of the edge view images were filtered to obtain the lattice line according to the image processing procedures detailed in Sosinsky et al., (1988) but with the following improvement. Membranes were corrected for curvature before the numerical filter mask was applied with a spline-fitting algorithm that was originally used to straighten filamentous helical particles (Egelman, 1986). The lattice lines seen in the Fourier transforms of these edge views become much stronger and narrower after computational straightening of the membranes in the digitized images.

Results

We tested various conditions to assess both the percentage of split junctions and the integrity of the membranes. Variables included two different isolation procedures for the initial starting material, urea concentration, pH, reducing agents, chelating agents, temperature, and length of incubation. We used thin sections of fixed and embedded pellets as our assay for the quality and quantity of split junctions. We assessed the efficiency of splitting by scoring micrographs for numbers of single membranes (split junctions), double membranes (intact junctions), and partially split gap junctions. In typical miniexperiments, 500–1500 total membranes were counted. Fig. 2*A* shows an electron micrograph of a thin section of one of our starting gap junction preparations. A typical "good" split junction preparation is shown in Fig. 2*B*, while Fig. 2*C* contains an example of a poorly split junction preparation. We used conventional negative stain and electron microscopy to ascertain how disruptive the treatments were on the in-plane lattice structure. Fig. 3*A* shows an electron micrograph of a gap junction preparation stained with 2% uranyl acetate. A micrograph of split junction is shown in Fig. 3*B*, and Fig. 3*C* shows a partially split junction. In general, split junctions tend to be smaller than intact gap junctions. The difference in plaque size may be due to an increased fragility of the membranes after urea treatment resulting in fracturing along domain boundaries. A summary of previously published protocols for splitting gap junctions is listed in Table 1. Table 2 summarizes the conditions we investigated for splitting gap junctions.

Quality and Efficiencies of Various Splitting Conditions

Two isolation protocols were used for isolating gap junctions. The major difference between the two protocols is the agent of solubilization of the nongap junctional membranes in the plasma membranes fraction. The first protocol was devised by Hertzberg (1984) and uses an alkali incubation while the second procedure uses detergents (Sarkosyl and Brij 58) to solubilize nonjunctional material (Fallon & Goodenough, 1981; Baker et al., 1985). Starting with 36 livers obtained from 3–4 week old rats (total tissue mass of 90–120 g), we found that we had more protein in our starting material when we used the Hertzberg protocol (~2.0 mg/ml) than when we used the Fallon and Goodenough protocol (~0.1 mg/ml). However, as determined by gel electrophoresis and electron microscopy, the detergent protocol gave purer and more crystalline junctions than the alkali extraction procedure. Since we obtained more starting material with the Hertzberg procedure, we used this method for surveying splitting conditions and then we used the Fallon and Goodenough procedure for refining conditions and isolating split junctions for structural analysis. The quality and the efficiency with which junctions were split were always better when the starting material was prepared with the detergent protocol than with the alkali procedure. Gap junctions prepared by the alkali procedure have larger lattice constants than those prepared by the detergent method (Hertzberg, 1984). Gap junction lattices with larger lattice constants presumably contain a higher lipid content. This finding indicates that the protein-to-lipid ratio in the sample may be an important factor in controlling the interaction of urea with connexins.

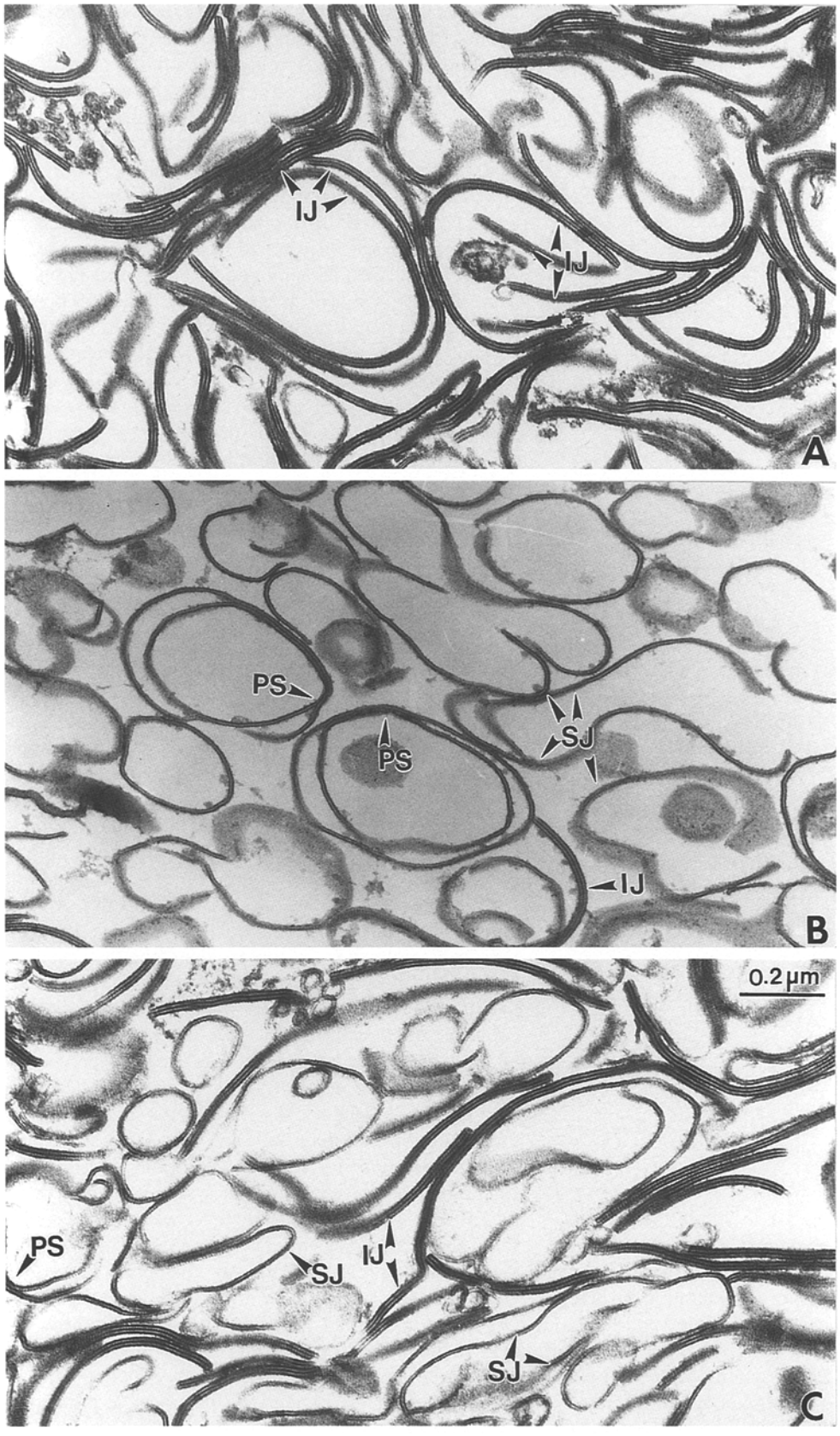

Fig. 2. Assessment of splitting protocols by ultramicrotomy of split junction pellets. Three representative micrographs are shown from (*A*) a preparation of gap junctions, (*B*) a preparation obtained when EGTA was included in the urea buffer and (*C*) a sample obtained under the same conditions as (*B*) except that EGTA was not in the buffer. The efficiency of splitting was greatly improved by the addition of EGTA to the urea buffer. Examples are shown on these micrographs of intact junctions (IJ), split junctions (SJ), and partially split gap junctions (PS).

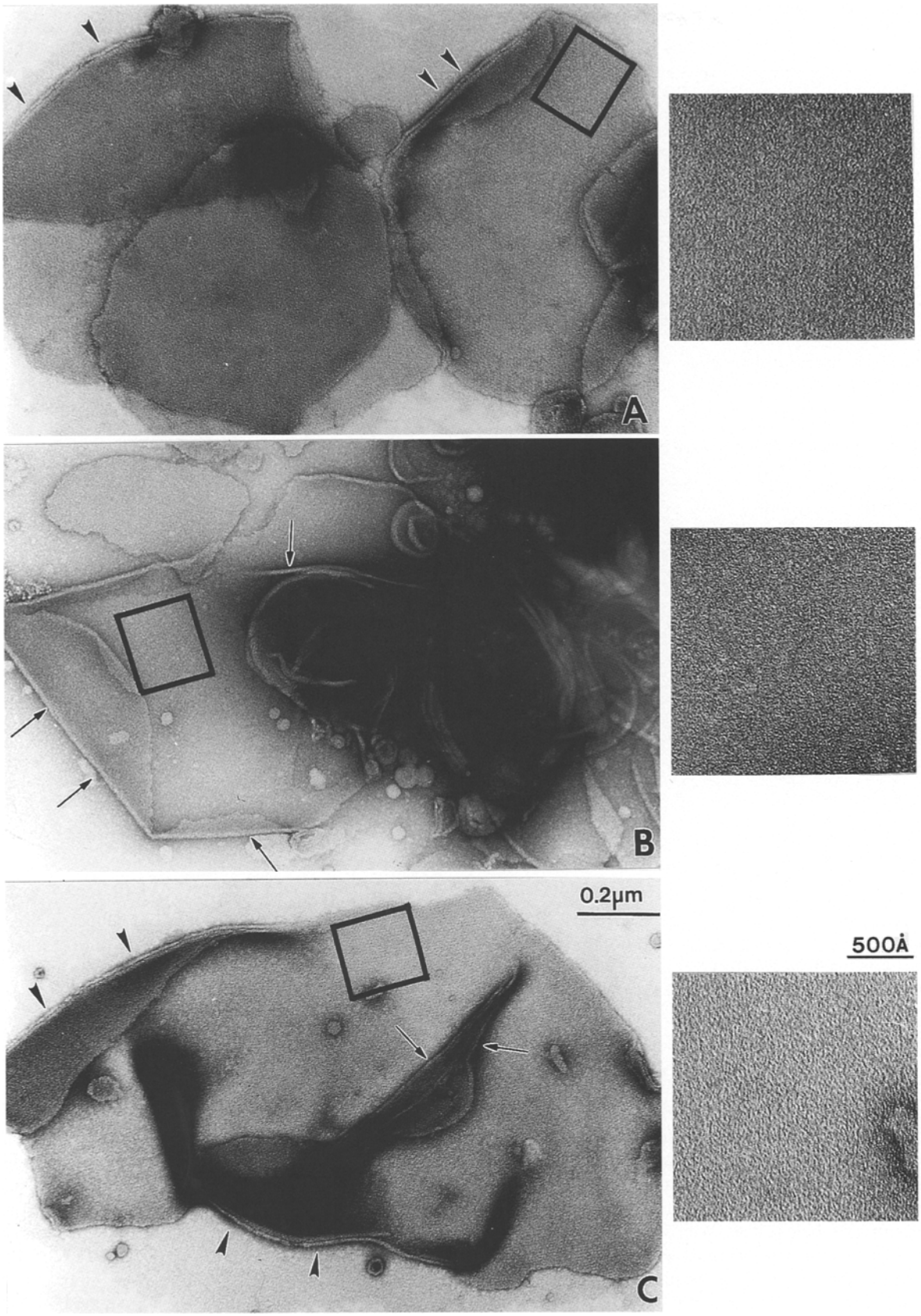

Fig. 3. *En face* views showing hexagonal lattice structure. These membrane structures have been stained with 2% uranyl acetate and examined under conventional imaging conditions. Examples of (*A*) intact gap junctions, (*B*) split junctions and (*C*) a partially split gap junction are shown. The arrowheads point to folds in the membrane indicative of the double membrane structure, while arrows point folds indicative of a single membrane. The connexons are held within a hexagonal lattice as shown by the higher magnification view of the boxed area in each image in the right-hand column.

Table 1. Published conditions used for splitting of gap junctions

Conditions	Reference	Comments
8 M urea, pH 10	(1) Manjunath et al., 1984 (2) Goodenough et al., 1988	original splitting procedure membrane structure intact, but amount split varies from sample to sample
0.1% SDS, pH 7.5	(1) Manjunath et al., 1984	intact junctions were first cross-linked with 5% glutaraldehyde. Membranes were all partially split
8 M urea, pH 12	(1) Zimmer et al., 1987 (1) Milks et al., 1988	same results as 8 M urea, pH 10
pH 2	(1) Zimmer et al., 1987	100% split junctions, but severe membrane disruption
8 M urea, pH 12.3 8 M urea, pH 7.2	(1) Zhang & Nicholson, 1994	variable splitting with alkaline pH; minimal splitting with neutral pH
Hypotonic sucrose (intact cells)	Goodenough et al., 1974 Goodenough et al., 1988	only used on hepatocytes

(1) indicates that starting material was obtained with the alkali extraction procedure (Hertzberg, 1984) while (2) represents gap junctions isolated with the detergent protocol (Fallon & Goodenough, 1981).

Table 2. Conditions used for splitting of gap junctions in this study

Protocol	Urea (M)	pH	DTT (mM)	Chelator (mM)	#1 Time/Temp (hr/°C)	#2 Time/Temp (days/°C)	Comments
[a]2	4	8			3/37	3–5/4	variable from prep to prep
1,2	4	8	5		3/37	3–5/4	no improvement from [a]
1,2	4	8	5		3/60	3–5/4	no improvement from [a]
[b]2	4	8	5	EGTA 1,3,5.5	3/37	3–5/4	consistently good (>15% improvement in junctions split)
2	4	3	5		3/37	3–5/4	all split but membrane structure disrupted
2	4	8	5	EGTA 3	3/25	3–5/4	poor splitting
2	4	8	5	EGTA 3	6/37	3–5/4	membrane structure disrupted
1,2	2	8	5		3/37	3–5/4	poor splitting
2	5	8	5	EGTA 3	3/37	3–5/4	good splitting (~80%)
2	4	8	5	EDTA 3	3/37	3–5/4	no improvement from [a]
1	4	8	5		3/37		no improvement from [a]
1	4	10	5		3/37	3–5/4	no improvement from [a]
1	4	8	5		1/60		no improvement from [a]
1	4	8	5		3/37		no improvement from [a]
1	4	8	5		6/37		membrane structure disrupted
1	4	8	5		6,12/37		membrane structure disrupted
1	4	8	5		6,12/60		membrane structure disrupted

All concentrations listed in this table are final concentrations after mixing of buffers and samples. (1) indicates that starting material was obtained with the alkali extraction procedure (Hertzberg, 1984) while (2) represents gap junctions isolated with the detergent protocol (Fallon & Goodenough, 1981). [a] indicates original starting conditions while [b] indicates conditions for our most successful urea treatment.

Previous published protocols for splitting junctions used incubations with 8 M urea. We were interested in trying to use urea at lower concentrations, i.e., under less harsh conditions, to break the hydrophobic interactions between connexons. To minimize exposure to high urea concentrations, we mixed our starting material by rapidly adding a urea buffer followed by vortexing to obtain a final concentration below 8 M. We found that 4 M urea was sufficient to split gap junctions with a yield of 40–90% single membranes within a sample. While 5 M urea yielded similar results to 4 M urea, the splitting efficiency decreased to less than 30% when 2 M urea was used.

High temperatures (37°C or 60°C) split junctions effectively when samples were incubated for 3 hr, but incubations for longer periods of time ($\geq$6 hr) either fragmented the membrane into smaller pieces with an accompanying loss of the hexagonal lattice or resulted in a "bubbled" appearance (*c.f.* Fig. 8 in Zimmer et al., 1987 or Fig. 7*B* in Zhang and Nicholson (1994) for similar micrographs). Gap junctions incubated under similar conditions at room temperature split poorly (42% of the membranes observed was split junctions) as opposed to the control sample kept at 37°C (which contained 62% split junctions). For unknown reasons, the integrity of

Table 3. Quantitative assessment of split junctions produced with chelating agents in the splitting buffer

Expt. (Prep Name)	% Singles	% Doubles	% Partials
+/– 1 mM EGTA (Z7)	90/60	6/33	4/7
+/– 1 mM EGTA (Z8)	43/52	53/43	4/5
+/– 1 mM EGTA (Z9)	75/53	21/44	4/3
+/– 5 mM EGTA (Z9)	66/53	31/44	3/3
+/– 5 mM EGTA (AA3)	81/67	18/32	1/1
+/– 5 mM EGTA (AA4)	78/31	20/67	2/2
+/– 5 mM EGTA (AA7)	62/40	32/57	6/3

Micrographs of thin sections of split junction preparations were scored for the numbers of intact junctions (double membrane structures), single membranes, and partially split gap junctions. Typically, 500–1500 total membranes were counted. The numbers shown in this table reflect the percentage of each species of membranes in the total population. In six of seven experiments, we found that the splitting efficiency increased significantly with the addition of EGTA to the urea buffer.

the sample seemed to improve if the mixture was refrigerated after the high temperature incubation. Therefore we typically kept the samples at 4°C for 3 or more days.

In previous protocols for splitting junctions (*c.f.* Table 1), the sample was at ~pH 10. In our protocol, the final pH of the incubation mixture was ~8. We found a high splitting efficiency at this pH and the splitting efficiency did not improve significantly if the pH was raised to 9 or 10. Gap junctions were 100% split at pH 3, but the membranes broke up into smaller fragments and the membrane structure was distorted.

The reducing agent, dithiothreitol (DTT), was included in our experiments: however, we observed no great difference in the splitting efficiency for samples with and without DTT. This indicated that disulfide bonds were not involved in the pairing of connexons. It has been reported that the six cysteine residues in the E1 and E2 loops form at least one and possibly three disulfide bonds between the loops, but there are no disulfide bonds between connexin subunits or connexons (John & Revel, 1991, Rahman & Evans, 1991).

The Effect of Chelators on the Splitting of Gap Junctions

Of all the conditions surveyed for splitting gap junctions with urea, the one addition to the urea buffer that significantly improved the splitting efficiency was EGTA. The same gap junction preparations split with identical conditions for urea concentration, pH, length of incubation, temperature and DTT, showed significant improvement upon the addition of EGTA in the urea buffer (Table 3). The images shown in Figs. 2*B*, and 3*B* are from samples which contained EGTA in the splitting buffer, while the urea buffer used for splitting the samples shown in Figs. 2*C* and 3*C* did not contain EGTA. We found an increase in the number of split junctions in 6 out of the 7 paired experiments (with and without EGTA) with 7 different starting preparations of intact junctions. In general, for samples with EGTA there is an increase of 15 to 30% in splitting efficiency compared to the control sample. Two other independent samples for which EGTA was included but no control samples were available contained 85 and 90% split junctions. There was no significant difference in the percentage of partially split junctions between plus and minus EGTA samples in all seven experiments. Two samples incubated with 5 mM EDTA contained 53% and 31% split junctions indicating that there was no improvement with the addition of EDTA to the urea buffer. EGTA is much more specific for chelation of Ca^{2+} than Mg^{2+} (Sillen, 1964). The binding constant of EGTA for Ca^{2+} is approximately one hundred times stronger than the binding constant of EDTA for Ca^{2+}. These results indicated that the binding of Ca^{2+} may have contributed to interactions that stabilized the docking of apposing connexons.

Protein Composition of Intact and Split Junctions

The primary connexin protein in rat liver gap junctions is Cx32. Cx26 is a minor component in rat liver gap junction preparations usually found at a ratio of ~1:10. As analyzed by SDS gel electrophoresis and immunoblotting and shown in Fig. 4, the protein composition of intact and split gap junction preparations was identical for the double membranes and the single connexon layers (Fig. 4*A*). Western blots with antibodies specific for cytoplasmic loop (C2 in schematic of Fig. 1*B*) amino acids 98–124 in Cx32 (Fig. 4*B*) and to C2 amino acids 108–122 of Cx26 (Fig. 4*C*) verified the presence and relative stoichiometries of these two proteins in the intact and split gap junction samples. Two antibodies generated against specific synthetic peptides to the cytoplasmic loop and one of the extracellular loops of Cx32 (Goodenough et al., 1988) and visualized by immunogold labeling and thin section EM bound to the split junction samples in similar amounts as reported in Goodenough et al., 1988 (*data not shown*). Therefore, the main action of the urea incubation was the separation of the two connexon layers and there was no gross rearrangement of the structure.

Split Junction Morphology

Split junctions can be easily seen in the thin section micrographs presented in Fig. 2. In the negatively stained *en face* views presented in Fig. 3, it was more difficult to distinguish between split junctions, intact junctions, and partially split gap junctions. However, by

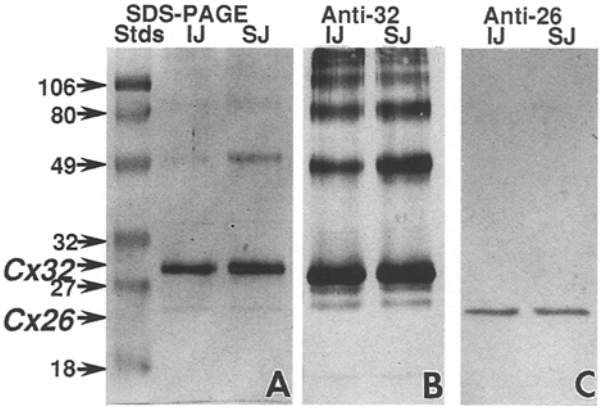

Fig. 4. Protein Composition. As judged by SDS gel electrophoresis, the connexin composition in rat liver plaques is ~1:10 in Cx26:Cx32. (*A*) Coomassie stained SDS gel containing a preparation of intact junctions (IJ, middle lane) and a sample of split junctions (SJ, right lane). The split junctions were prepared from the sample of intact junctions shown in this gel. Protein molecular weight standards are shown in the left hand lane. All molecular weights are in kDa. These preparations have been Western blotted with two antibodies, one which is specific for amino acids 98–124 of the C1 loop of Cx32 (Fig. *B*) and the other which recognizes amino acids 108–122 of the C1 loop Cx26 (Fig. *C*). The higher molecular weight species in the anti-Cx32 Western Blots are aggregates of Cx32. The banding pattern is the same for intact and split junctions indicating that there is no change in the protein composition between the two samples.

examination of folds in the membrane, one could usually ascertain the thickness of the membrane. For example, arrowheads in Fig. 3*A* point to folds in double membrane structures where the two bilayers can be distinguished. The arrows in Fig. 3*B* illustrate folds in split junctions indicating single bilayers. The membrane shown in Fig. 3*C* is most likely a partially split gap junction because it contains double-layer folds and single-layer folds. In each case, the hexagonal lattice structure was maintained. The lattice structure is shown in the enlargements of the boxed areas to the right of the low power micrographs (Fig. 3).

There was an asymmetry to the connexon morphology which was evident upon splitting. Inspection of electron micrographs of thin sections of membranes revealed that the tannic acid fixation emphasized a "fuzzy coat" on the cytoplasmic surface, as indicated in Fig. 5 by the notation "FC", which is not evident on similar specimens fixed without tannic acid (Caspar et al., 1977). The difference in staining of the cytoplasmic and extracellular surfaces can be seen in the sections of a split junction and a partially split junction (Fig. 5*B* and *C*). An image of thin sections through intact junctions is shown for comparison. The spacing of the lattice lines (~1/73 $Å^{-1}$) in the Fourier transforms shown in Fig. 6 indicated that the lattice constant was the same for the single connexon layers and intact gap junctions. In the image processed sections, stain delineated the channel and collected between the connexons (in the extracellular surface) in both the single and double membrane structures. In the images of split junction cross-sections, the extracellular surface of the split junction appeared scalloped.

Cryo-Electron Microscopy of Single Connexon Layers

The difference in mass density between intact and split junctions could be seen in unstained frozen hydrated samples. The same morphological guides, e.g., folds and appearance of edges, for distinguishing between intact junctions and split junctions applied to samples suspended in vitreous ice. The micrograph in Fig. 7*A* is an example of a split junction suspended in vitreous ice. The folds in the membrane are apparent. A higher magnification view (Fig. 7*B*) shows that the connexons are still maintained within the hexagonal lattice and one can sight down the lattice rows in the direction of the arrowheads in Fig. 7*B*. Fortuitous curling of the membrane edges reveal the bilayer profile (*see* arrows).

The boxed area of the image of Fig. 7*C* was chosen because its diffraction pattern contained visible spots at the (3, 0) range of resolution (~25 Å). The connexons were visible in the original image as black doughnuts. The lattice constant for this image was 82.8 Å, which was typical of previous gap junction preparations (Baker et al., 1985). The correlation average, which is the sum of 100 areas containing a central connexon and portions of its six neighbors, is shown in Fig. 7*E*. The reference used to generate this average was selected from a filtered image of the same area. The filtered image had been locally averaged to enhance the lattice structure and high and low pass filtered to remove extraneous noise at very low and high resolution. The resolution of the correlation average according to the spectral signal-to-noise criterion of Unser, Trus & Steven (1991) is ~16–18 Å.

The availability of split gap junctions allowed examination of single connexons in projection. We wanted to confirm the hexagonal substructure demonstrated in isolated connexons by Stauffer et al., 1991. To this end, a rotational power spectrum analysis (Crowther & Amos, 1971) of the Bessel order harmonics, which is a measure of rotational symmetry, of the central connexon in the correlation average revealed that about ~35% of the azimuthal power is 6-fold, while only 5% is 5-fold. Thus, the structure of the connexon in the split junction was highly hexagonal. As a test to show that the reference had not introduced a hexagonal bias into the average, another reference was constructed which was a single doughnut with the same approximate dimensions as the connexons in the image. Correlation averages summed from either 100 to 50 areas contained approximately the same 6- and 5-fold azimuthal power as the correlation

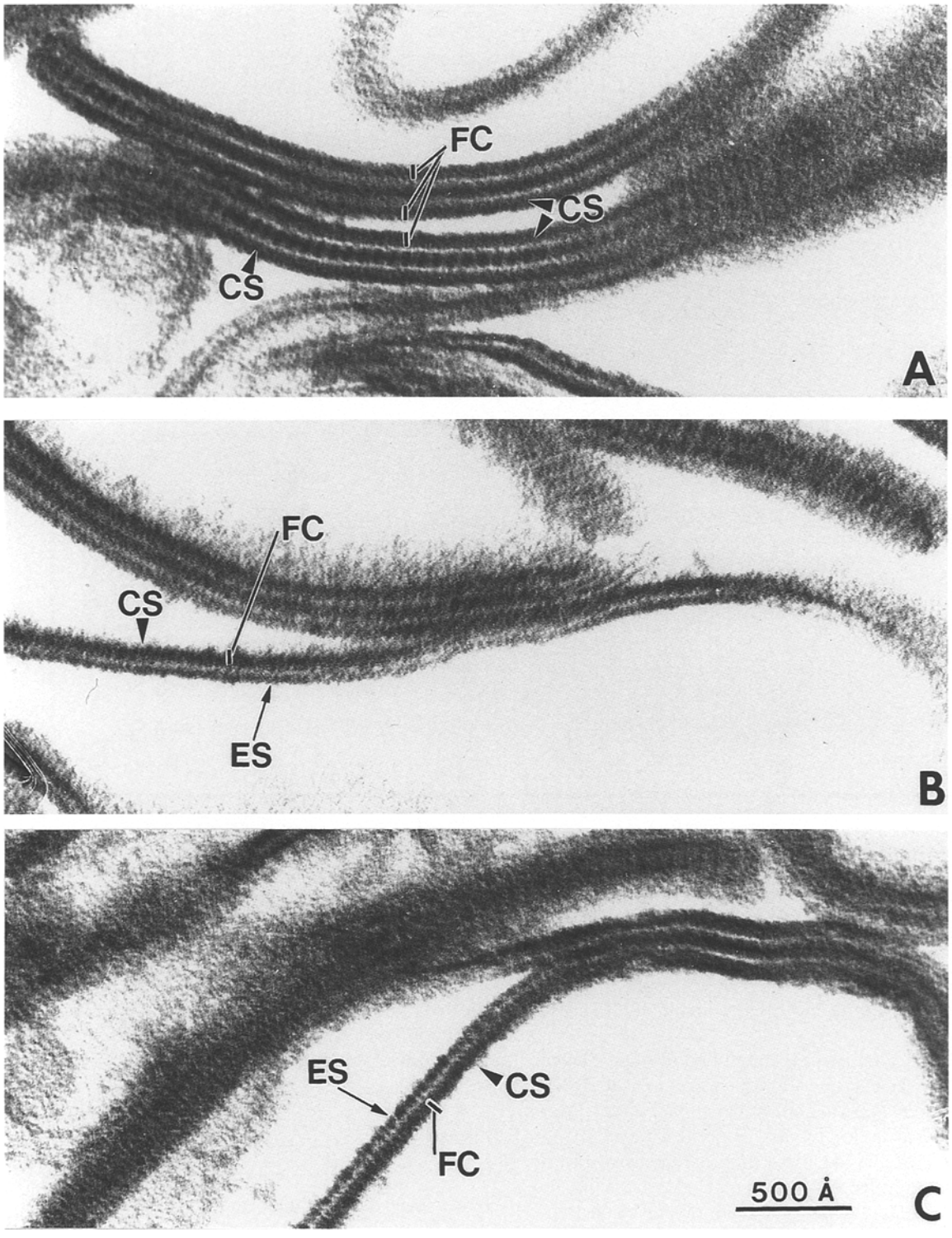

Fig. 5. Differential staining of the cytoplasmic and extracellular surfaces in thin section electron micrographs. Higher magnification views of thin sections through intact junctions (*A*), a split junction (*B*) and a partially split junction show thicker layers of positive stain on the cytoplasmic surfaces (CS) than the extracellular surface (ES). The larger protein domains localized to the cytoplasmic surface are disordered and these domains may be selectively enhanced by the positive stain. This thick layer of stain is referred to as the "fuzzy coat" and denoted by the bar marked FC.

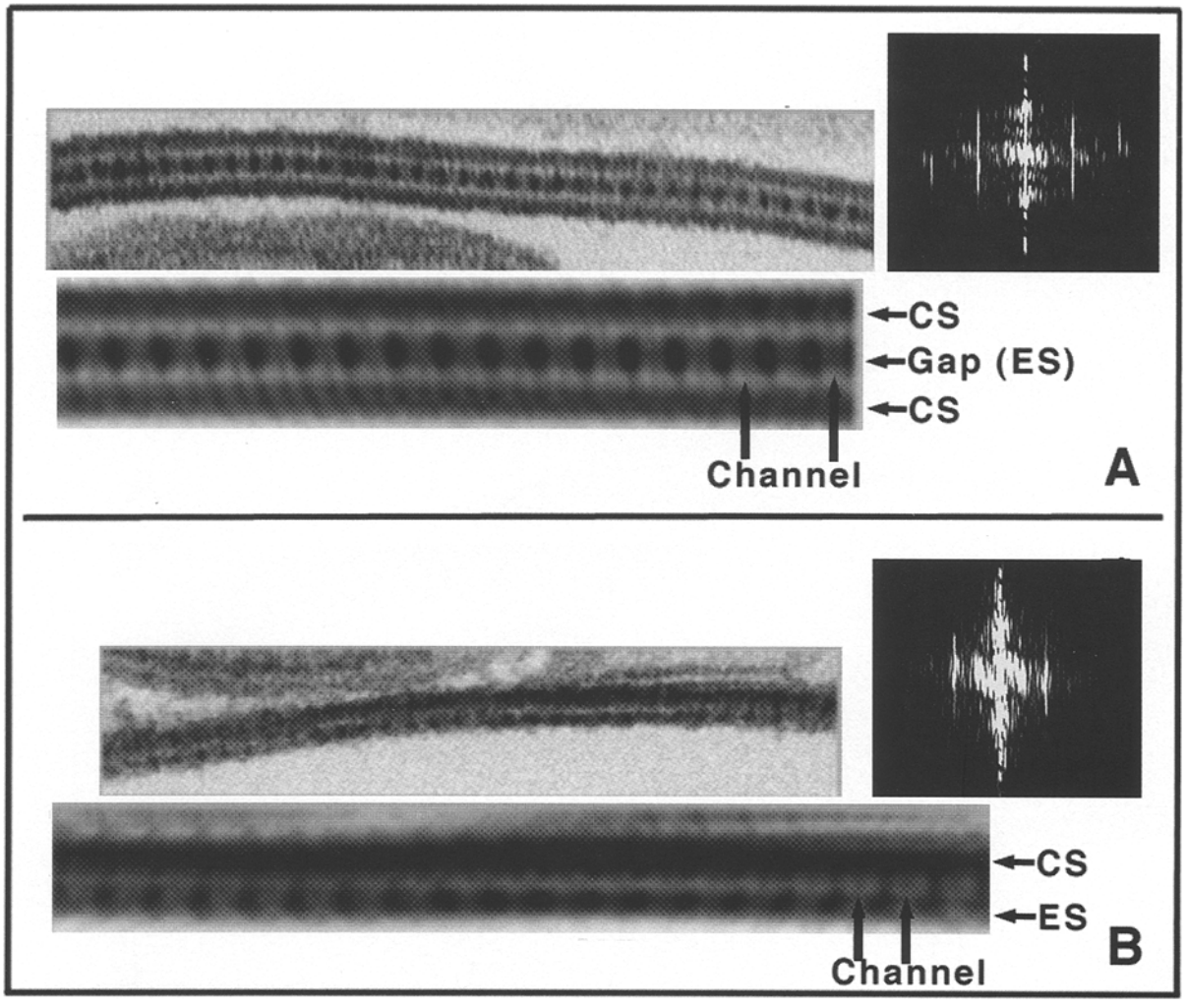

Fig. 6. Sections along the lattice axes showing the connexon structure perpendicular to the membrane plane. The inplane lattice structure is not grossly disturbed by splitting of the membranes with urea and EGTA. This is shown by the same spacings of lattice lines in the computed diffraction patterns between (*A*) an intact junction and (*B*) a split junction. The original images as shown in the top image of each panel and have been corrected for curvature and filtered with a numerical layer line mask. The filtered image is shown below the original at twice the magnification. The cytoplasmic surfaces (CS) and extracellular surfaces (ES) are indicated as is the stain filled channel. Note the scallopped appearance of the ES in the split junction images in panel B.

average generated with the filtered image as the reference.

The 6-fold symmetrized correlation average, shown in Fig. 7*F*, is skewed by ~8°, which is similar to previously reported reconstructions of whole junctions (Baker et al., 1983; Baker et al., 1985; Gogol & Unwin, 1988). This skewing can be identified from the intensity difference between the (2, 1) and (1, 2) reflections in the diffraction patterns. The color table of the reconstructions has been inversed from the original image such that white corresponds to the highest density material, (protein), while black corresponds to low density scattering (ice in the central channel of the connexon). The scattering for the lipid bilayer was contained in the middle grey levels. The strong scattering of the channel was reflected in the increased strength of the (2, 0) set of diffraction spots relative to the (1, 0). This was typical of frozen-hydrated intact junctions as well.

Discussion

Hydrophobic Interactions between Paired Connexons

Formation of the membrane pair requires a tight seal at the contact points between the two connexons. As pointed out by Peracchia et al. (1994), the binding of the two connexons must be sufficiently strong to create an insulated channel. Hydrophobic interactions must be the

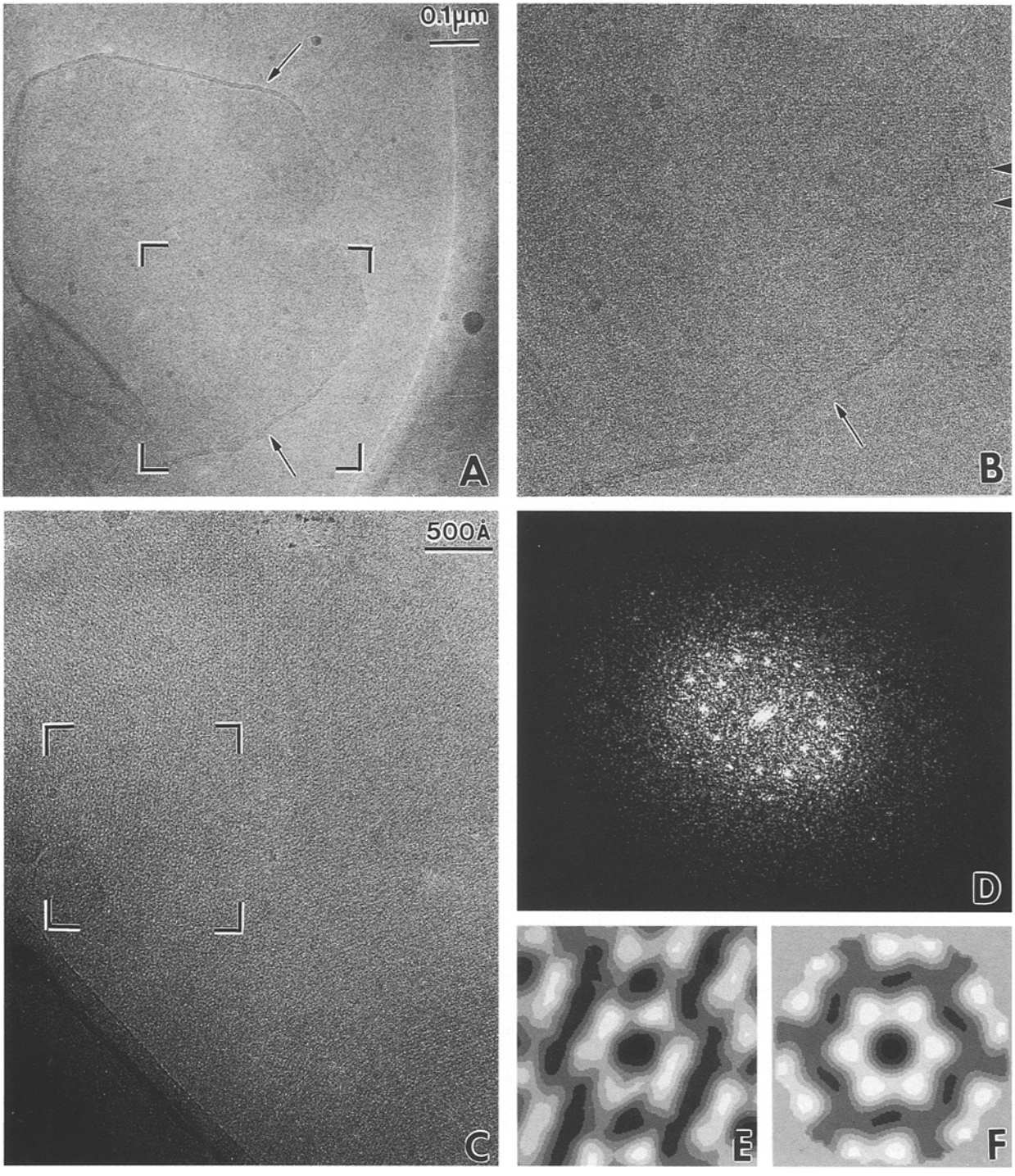

Fig. 7. Cryoelectron micrographs of intact and split junctions. (*A*) Image of a frozen-hydrated split junction suspended in vitreous ice over a holey carbon film. The arrows points to folds showing the double membrane structure. (*B*) Enlargement of the boxed area shown in *A*. The magnification of *B* is twice that of *A* (360,000×). The arrow points to the single membrane profile, indicating that this is a split junction. The arrowheads point down one of the lattice directions of the hexagonally packed connexons. (*C*) An image of a portion of a frozen hydrated split junction suspended over a hole. The connexons are black in the original images. The diffraction pattern of the boxed area of this image is shown in (*B*) while the correlation average from averaging 100 areas containing one central connexon plus approximately half of its six nearest neighbors is shown in (*E*). The reconstruction shown in (*F*) is the sixfold rotational average of the correlation average (*E*). The contrast has been reversed in (*E*) and (*F*) so that protein appears white and ice appears black. These reconstructions are displayed with seven gray levels.

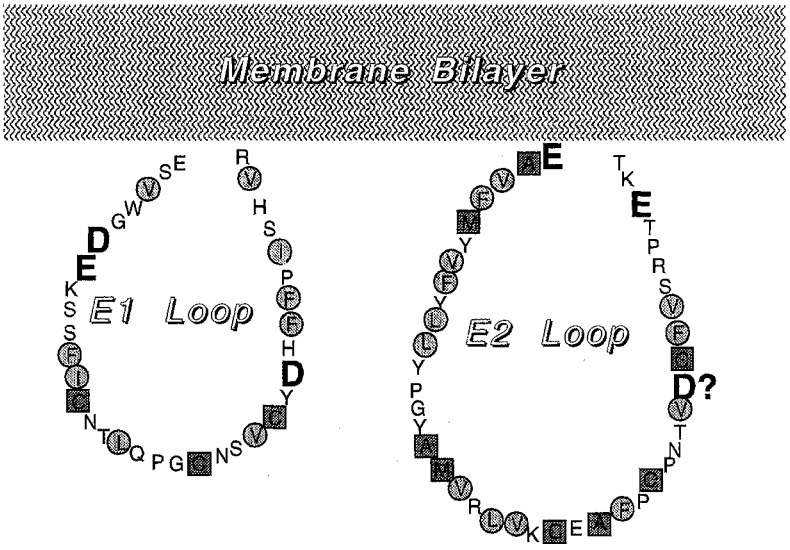

Fig. 8. Primary amino acid sequences of the two extracellular loops. The sequences of the E1 and E2 loops are shown here in a highly schematized drawing. The assignment of these loops has been adapted from Peracchia et al. (1994). Amongst 16 connexins, 5 strictly conserved aspartic and glutamic acid residues are shown in large bold letters. One aspartic acid residue in the E2 loop is conserved in 14 out of 16 connexins and is indicated with a ?. Strongly hydrophobic residues (I, V, L, and F) are indicated by the lighter gray circle while weakly hydrophobic residues (C, M, and A) are highlighted in darker gray squares (assignments according to Kyte and Doolittle, 1982).

predominant force at the contact regions of the apposing connexons since a chaotropic agent such as urea is absolutely necessary to split gap junctions into two separate membranes. Gap junctions are extremely stable in the same buffers in the absence of urea (5 mM Tris or 5 mM Tris-5 mM EGTA). In our experiments, other factors such as elevated temperatures in the presence of urea also significantly increase the splitting efficiency. Short incubations (1–3 hours) at the higher temperatures may break these interconnexon hydrophobic interactions, while longer incubations (≥6 hr) at elevated temperatures may start to disrupt secondary structure. The incubations at 37°C are at physiological temperatures and would not be expected to impact lipid-protein interactions. However, incubations at 4°C may lead to rearrangements of the surrounding lipids within the lattice.

Close inspection of the amino acid sequence for the extracellular loops, E1 and E2 (shown in Fig. 8), suggests that there are significant stretches of hydrophobic residues. If one includes both strongly (I, V, F, and L) and weakly (C, M, and A) hydrophobic amino acids (Kyte & Doolittle, 1982), the E1 loop in Cx32 contains 12 hydrophobic residues of the 35 amino acids, while 21 out of the 43 amino acids in the E2 loop are hydrophobic (Fig. 8). If tyrosine is also considered highly hydrophobic (Nozaki & Tanford, 1971) then there is a stretch of 11 consecutive hydrophobic amino acids in the E2 loop. This is remarkable considering that this portion of the sequence is localized to the aqueous gap region. This sequence of eleven E2 amino acids is a candidate for domains involved in specific connexon-connexon interactions. Recently, White et al. (1994) have shown selectivity in functional heterotypic channel formation in paired *Xenopus* oocytes. This selectivity can be conferred on a nonselective connexin by exchanging E2 domains. These findings imply that the E2 loop is an important determinant in the compatability between connexins.

Urea was effective in splitting junctions under milder conditions than previously reported. The single connexon layers still maintained their structural integrity. The quantity and quality of split junctions depended on the method used to prepare the starting material. This may indicate that the protein/lipid ratios were important. Gap junctions with higher protein/lipid ratios, as determined by smaller lattice constants such as those prepared with detergents, split more efficiently than gap junctions obtained by alkali extraction.

The primary action of denaturants such as urea and guanidine hydrochloride at high concentrations is thought to be the unfolding of proteins (Timasheff, 1993). At lower concentrations, the denaturant acts as a cosolvent and binds to the protein before it unfolds (Timasheff, 1993). In the case of gap junctions, the effect of urea may be to solvate the hydrophobic residues responsible for the sealing of the channel. Since we can remove the split junctions from the urea and resuspend them in Tris buffers, it is likely that either there are conformation changes of these hydrophobic residues that bury them from the aqueous environment or that some residual urea is bound to solvate these residues. Goodenough et al. (1988) reported a decrease in the accessibility of the extracellular loops to E2 specific antibodies with time when gap junctions were split in intact hepatocytes with hypotonic sucrose, implying conformational changes subsequent to junctional splitting.

Effect of Ca^{2+} on Stability of the Connexon Pair

EGTA significantly increased the efficiency of splitting. Since EGTA is specific for chelation of Ca^{2+}, the binding

of Ca^{2+} may contribute to interactions that stabilize the docking of apposing connexons confirming some early observations by Peracchia (1977). Connexins contain 2 aspartic and 3 glutamic acid residues in the two extracellular loops which are absolutely conserved between various connexins (Peracchia et al., 1994). A third aspartic acid residue is conserved in the primary sequences of 14 out of 16 connexins. These amino acids are likely sites for divalent cation binding (Chakrabarti, 1990). Gap junctions are 100% split at low pH where those amino acids are neutralized but the membrane structure is severely damaged (Zimmer et al., 1987, this study).

Unwin and his coworkers (Unwin & Zampighi, 1980; Unwin & Ennis, 1984) have reported that removal of Ca^{2+} by EGTA caused a slight rearrangement of the subunits in the hexamer in their three-dimensional reconstructions. While this was originally interpreted as a conformational change for gating, based on the effect that we see, it is possible that the loss of calcium ions induces a rearrangement of the extracellular loops which may cause packing changes.

Structure of Individual Connexons

The main action of the urea incubation is to separate the two connexon layers. The connexons are maintained within the hexagonal lattice with the same lattice constant and packing of the whole junctions. As seen in Fig. 5, there is an asymmetry in the single layers. The stain is much thicker on the cytoplasmic surfaces than on the gap side and the extracellular surface of the connexon has a scalloped edge. We see the same urea insensitive "fuzzy coat" as was seen in thin sections of cardiac junctions (Manjunath et al., 1985). Since this "fuzzy coat" was absent in proteolyzed cardiac junctions, it was postulated that there was selective enhancement of the cytoplasmic domains. Close inspection of the filtered images of sections shown in Fig. 6 reveal possible protein extrusions which could correspond to the flexible cytoplasmic domains of Cx32 and Cx26.

While it has been postulated that the cytoplasmic domains are flexible and therefore, invisible to image averaging techniques, the opposite is true of the extracellular surface (Sosinsky, 1992; Hoh et al., 1993). The transmembrane and extracellular domains of the connexon are the most ordered parts of the structure. It is this rigidity that made the extracellular surface of the gap junction an amenable specimen for atomic force microscopy (Hoh et al., 1993). The images of Hoh et al. (1993) are intriguing because of the topological detail of the extracellular surface. These images suggest that two apposing connexons fit into one another in the same fashion as intermeshing cogs. Such a topology would be an important factor in the molecular recognition of two hemichannels. In the views perpendicular to the membrane surface, we see a scallopped appearance rather than a flat edge at the part of the connexon that would dock with another connexon. Confirmation of this modulated molecular architecture of the extracellular surface awaits a three-dimensional reconstruction from single connexon layers.

The antibodies used to analyze the protein composition in our samples were the generous gift of Dr. David Paul. We thank Dr. Camillo Peracchia for sending us a preprint of his chapter on molecular mechanisms of connexon gating and docking which helped guide our thinking about interconnexon forces and John Badger for information on divalent cation sites in protein structure. We thank Amani Thomas-Yusuf for technical assistance. The photographic expertise of Marie Craig is gratefully acknowledged. This work was funded by National Institutes of Health GM43217 to G.E.S. and GM18974 to D.A.G.

References

Baker, T.S., Caspar, D.L.D., Hollingshead, C.J., Goodenough, D.A. 1983. Gap junction structures. IV. Asymmetric features revealed by low-irradiation microscopy. *J. Cell Biol.* **96**:204–216.

Baker, T.S., Sosinsky, G.E., Caspar, D.L.D., Gall, C., Goodenough, D.A. 1985. Gap junction structures VII. Analysis of connexon images obtained with cationic and anionic negative stains. *J. Mol. Biol.* **184**:81–98.

Barr, L., Dewey, M.M., Berger, W. 1965. Propagation of action potentials and the structure of the nexus in cardiac muscle. *J. Gen. Physiol.* **48**:797–823

Bennett, M.V.L., Barrio, L.C., Bargiello, T.A., Spray, D.C., Hertzberg, E., Saez, J.C. 1991. Gap junctions: new tools, new answers, new questions. *Neuron* **6**:305–320

Bennett, M.V.L., Goodenough, D.A. 1978. Gap junctions, electronic coupling, and intercellular communications. *Neurosci. Res. Prog. Bull.* **16**:375–486

Caspar, D.L.D., Goodenough, D.A., Makowski, L., Phillips, W.C. 1977. Gap junctions structures I. Correlated electron microscopy and x-ray diffraction. *J. Cell Biol.* **74**:605–628

Chakrabarti, P. 1990. Interaction of metal ions with carboxylic and carboxamide groups in protein structures. *Prot. Engin.* **4**:49–56

Crowther, R.A., Amos, L.A. 1971. Harmonic analysis of electron microscope images with rotational symmetry. *J. Mol. Biol.* **184**:81–98

Dahl, G., Miller, T., Paul, D., Voellmy, R., Werner, R. 1987. Expression of functional cell-to-cell channels from cloned rat liver gap junction complementary DNA. *Science* **236**:1290–1293

Dermietzel, R., Hwang, T.K., Spray, D.S. 1990. The gap junction family: structure, function, and chemistry. *Anat. Embryol.* **182**:517–528

Dubochet, J., Adrian, M., Chang, J.J., Homo, J.C., Lepault, J., MacDowall, A.W., Shultz, P. 1988. Cryo-electron microscopy of vitrified specimens. *Quart. Rev. Biophys.* **21**:129–228

Egelman, E.H. 1986. An algorithm for straightening images of curved filamentous structures. *Ultramicros.* **19**:367–374

Fallon, R.F., Goodenough, D.A. 1981. Five-hour half-life of mouse liver gap junction protein. *J. Cell Biol.* **90**:521–526

Francis, N.R., Irikura, V.M., Yamaguichi, S., DeRosier, D.J., Macnab, R.M. 1992. Localization of the *Salmonella typhiumurium* flagellar switch protein FliG to the cytoplasmic M-ring face of the basal body. *Proc. Natl. Acad. Sci. USA* **89**:6304–6308

Goliger, J.A., Paul, D.L. 1994. Expression of gap junction proteins

Cx26, Cx31.1, Cx37, and Cx43 in developing and mature rat epidermis. *Devel. Dynam.* **200:**1–13

Gogol, E., Unwin, N. 1988. Organization of connexons in isolated rat liver gap junctions. *Biophys. J.* **54:**105–112

Goodenough, D.A., Gilula, N.B. 1974. The splitting of hepatocyte gap junctions and *Zonulae occludentes* with hypotonic disaccharides. *J. Cell Biol.* **61:**575–590

Goodenough, D.A., Paul, D.L., Jesaitis, L. 1988. Topological distribution of two connexin32 antigenic sites in intact and split rodent hepatocyte gap junctions. *J. Cell Biol.* **107:**1817–1824

Hertzberg, E.L. 1984. A detergent independent procedure for the isolation of gap junctions from rat liver. *J. Biol. Chem.* **259:**9936–9943

Hoh, J.H., Lal, R., John, S.A., Revel, J.-P., Arnsdorf, M.F. 1991. Atomic force microscopy and dissection of gap junctions. *Science* **235:**1405–1408

Hoh, J., Sosinsky, G.E., Revel, J.-P., Hansma, P.K. 1993. Structure of the extracellular surface of the gap junction by atomic force microscopy. *Biophys. J.* **65:**149–163

John, S.A., Revel, J.-P., 1991. Connexon integrity is maintained by non-covalent bonds: intramolecular disulfide bonds link the extracellular domains in rat connexon-43. *Biochem. Biophys. Res. Commun.* **178:**1312–1318

Kyte, J., Doolittle, R.F. 1982. A simple method for displaying the hydropathic character of a protein. *J. Mol. Biol.* **157:**105–132

Makowski, L. 1988. X-Ray diffraction studies of gap junction structure. *In:* Advances in Cell Biology 2. K. Miller, editor. pp. 119–158 JAI, New York

Makowski, L., Caspar, D.L.D., Phillips, W.C., Goodenough, D.A. 1977. Gap junction structure II. analysis of the X-Ray diffraction data. *J. Cell Biol.* **74:**629–645

Manjunath, C.K., Goings, G.E., Page, E. 1984. Detergent sensitivity and splitting of isolated liver gap junctions. *J. Membrane Biol.* **78:**147–155

Manjunath, D.K., Goings, G.E., Page, E. 1985. Proteolysis of cardiac gap junctions during their isolation from rat hearts. *J. Membrane Biol.* **85:**159–168

Milks, L.C., Kumar, N.M., Houghten, R., Unwin, N., Gilula, N.B. 1988. Topology of the 32-kd liver gap junction protein determined by site-directed antibody localizations. *EMBO J.* **7:**2967–2975

Nozaki, Y., Tanford, C. 1971. The solubility of amino acids and two glycine peptides in aqueous ethanol and dioxane solutions. *J. Biol. Chem.* **246:**2211–2217

Peracchia, C. 1977. Gap junctions. Structural changes after uncoupling procedures. *J. Cell Biol.* **72:**628–641

Peracchia, C., Lazrak, A., Peracchia, L.L. 1994. Molecular models of channel interaction and gating in gap junctions. *In:* Membrane Channels. Molecular and Cellular Physiology, C. Peracchia, editor, pp. 361–377. Academic, New York

Rahman, S., Evans, W.H. 1991. Topography of connexin 21 in rat-liver gap junctions—evidence for an intramolecular disulfide linkage connecting the 2 extracellular peptide loops. *J. Cell Sci.* **100:**567–578

Sikewar, S.S., Downing, K.H., Glaeser, R.M. 1991. Three-dimensional structure of an invertebrate intercellular communicating junction. *J. Struct. Biol.* **106:**255–263

Sikewar, S.S., Unwin, N. 1988. Three-dimensional structure of gap junctions in fragmented plasma membranes from rat liver. *Biophys. J.* **54:**113–119

Sillen, L.G. 1964. Stability constants of metal-ion complexes. Second Edition. Chemical Society (Great Britain) **17,** London, Chemical Society

Sosinsky, G.E. 1992. Image analysis of gap junction structures. *Electr. Microsc. Rev.* **3:**59–76

Sosinsky, G.E., Baker, T.S., Caspar, D.L.D., Goodenough, D.A. 1990. Correlation analysis of gap junction lattices. *Biophys. J.* **58:**1213–1226

Sosinsky, G.E., Jesior, J.C., Caspar, D.L.D., Goodenough, D.A. 1988. Gap junction structures VIII. Membrane cross-sections. *Biophys. J.* **53:**709–722

Stauffer, K.A., Kumar, N.M., Gilula, N.B., Unwin, N. 1991. Isolation and purification of gap junction channels. J. Cell Biol. **115:**141–150

Swenson, K.I., Jordan, J.R., Beyer, E.C., Paul, D.L. 1989. Formation of gap junctions by expressions of connexins in *Xenopus* Oocyte Pairs. *Cell* **57:**145–155

Timasheff, S.N. 1993. The control of protein stability and association by weak interactions with water: How do solvents affect these processes? *Annu. Rev. Biophys. Biomol. Struct.* **22:**67–97

Unser, M., Trus, B.L., Steven, A.C. 1987. A new resolution criterion based on spectral signal-to-noise ratios. *Ultramicros.* **23:**39–52

Unwin, P.N.T., P.D. Ennis. 1984. Two configurations of a channel-forming membrane protein. *Nature* **307:**609–613

Unwin, P.N.T., Zampighi, G. 1980. Structure of the junction between communicating cells. *Nature* **283:**545–549

White, T.W., Bruzzone, R., Wolfram, S., Paul, D.L., Goodenough, D.A. 1994. Selective interactions among multiple connexin proteins expressed in the vertebrate lens: the second extracellular domain is a determinant of compatibility between connexins. *J. Cell Biol.* **125:**879–892

Zhang, J.-T., Nicholson, B.J. 1994. The topological structure of connexin 26 and its distribution compared to connexin 32 in hepatic gap junctions. *J. Membrane Biol.* **139:**15–29

Zimmer, D.B., Green, C.R., Evans, W.H., Gilula, N.B. 1987. Topological analysis of the major protein in isolated intact rat liver gap junctions and gap junction-derived single membrane structures. *J. Biol. Chem.* **262:**7751–7763